INFN/AE–97/46–47
23 Luglio 1997

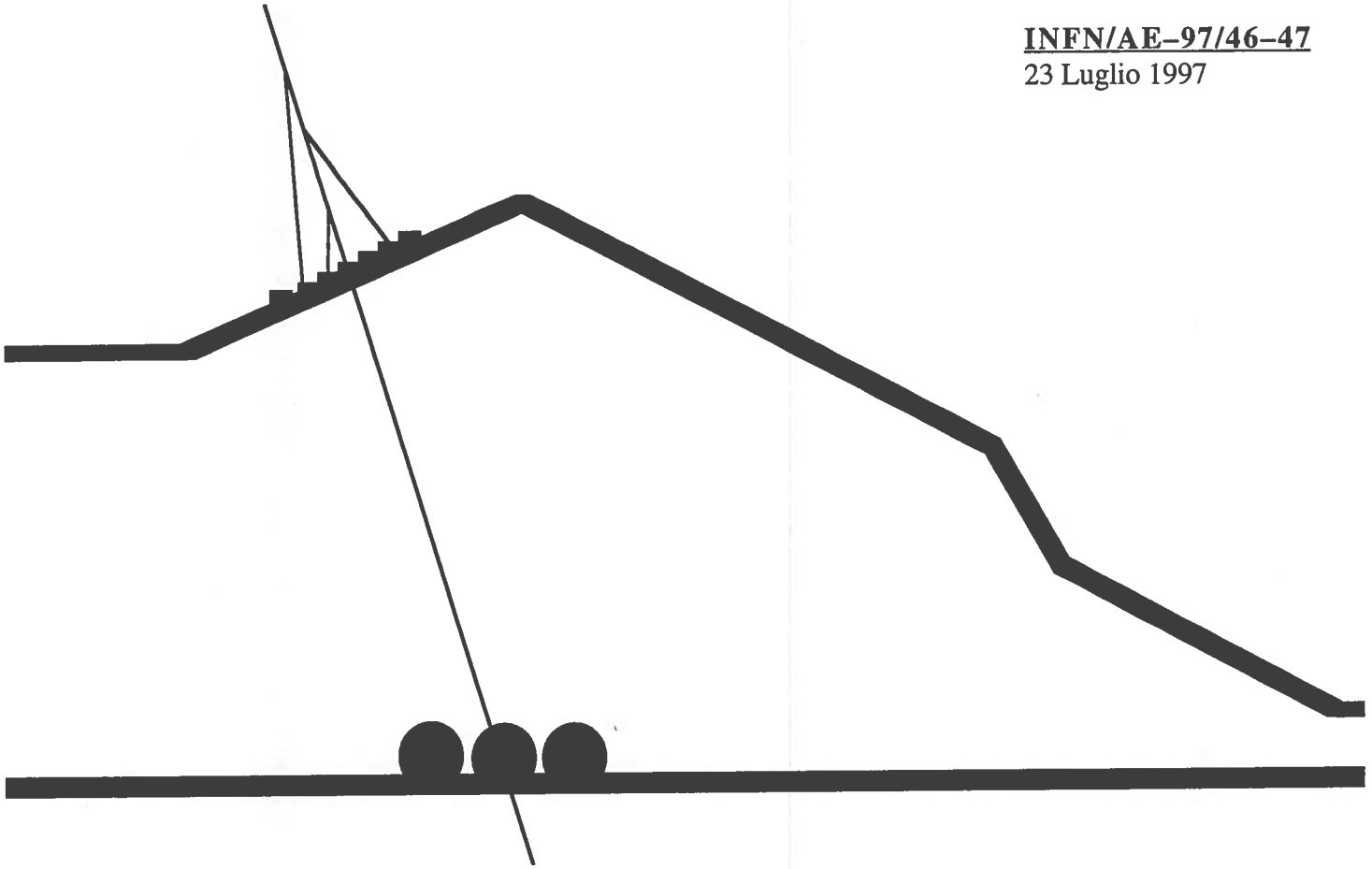

(Contributions of the MACRO and EAS TOP Collaborations to the XXV ICRC Durban, South Africa July 28-Aug10,1997)

INFN – Laboratori Nazionali del Gran Sasso

Published by ***SIS–Pubblicazioni*** *dei Laboratori Nazionali di Frascati*

STUDY OF THE PRIMARY COSMIC RAY COMPOSITION IN THE KNEE REGION WITH EAS-TOP AND MACRO

EAS–TOP and MACRO Collaborations

INFN/AE–97/46
23 Luglio 1997

ABSTRACT

The rigidity dependent model of the cosmic ray composition at the "knee" is checked by means of the combined EAS–TOP and MACRO data at the Gran Sasso laboratories. Different hadron interaction models provide consistent results with both the muon multiplicity and with the correlated electron and TeV muon data from the two experiments.

INTRODUCTION

The combined measurements of the e.m. component of EAS at the surface and of the high energy muons recorded in deep underground laboratories allow studies of both the cosmic ray primary composition and the interaction models used to interpret the data. Such measurements are performed by the EAS–TOP and MACRO detectors at the Gran Sasso Laboratories. EAS–TOP is the EAS array (enclosed area $A_i = 10^5$ m^2, sensitive area $A_s = 350$ m^2) measuring the shower size (total number of charged particles N_e) at 2000 m a.s.l., while MACRO samples the number of muons (N_μ) at a minimum rock depth of 3100 m w.e. ($A_s = 6 \times 140$ m^2, E_μ^{th}=1.3 TeV). The two detectors are separated by 1100–1300 m of rock and located at a relative zenith angle of $\sim 30°$. Details on the detectors and on their performances and on the analysis of a first sample of coincident data have been presented elsewhere (EAS–TOP and MACRO, 1990, 1993, 1994, 1995). In the present note we present an analysis of the muon multiplicity distributions in different intervals of shower size (below and above the knee) to test the Peters - Zatsepin rigidity dependent model of the knee ($E_k(Z)=Z \cdot E_k(1)$), as e.g. predicted by the rigidity dependent leakage effect from the Galaxy (Peters, 1959 and Zatsepin et al., 1962). Hadron interaction models based on different physical principles are used.

THE DATA

From the technical point of view, we want to stress the combined reconstruction capabilities of the two detectors. They are outlined in Fig. 1 where the differences in the projected arrival directions between the EAS (time-of-flight-technique) and muons (tracking technique) are shown. The distribution widths are compatible with the resolutions of both detectors ($\sim 1°$ each), while the mean values don't show any systematic effect at a level $< 0.05°$. Concerning the physics results, coincident events are selected in the range in which the shower size can be reconstructed by EAS–TOP. Data have been collected during 347.8 live days for a total number of 7889 events in the useful angular window. The number of recorded events is 1310 for $N_e \geq 2.2 \cdot 10^5$ and 226 for $N_e \geq 7 \cdot 10^5$ i.e. the size of the knee as observed at 30° (EAS–TOP collab., 1995), corresponding to about 2200 TeV for primary protons.

RESULTS AND CONCLUSIONS

The results are compared with simulations based on the HEMAS (Forti et al., 1990) and DPMJET (Battistoni et al., 1995 and Ranft, 1995) codes. Full descriptions of the detectors are included following the GEANT code (Brun et al., 1984). In the HEMAS code the interaction model is obtained by the parametrization of the UA5 experimental results at the SPS collider. The DPMJET code is based on the two component Dual Parton Model including the mini–jet production as predicted by the lowest order perturbative QCD, and is therefore a theoretically inspired model. An extrapolation of the low energy data is used for the primary composition (see Table 1), with different hypotheses about the knee: at constant primary energy ($E_k(Z)=E_k(1)$=2200 TeV), and at atomic number scaling energies ($E_k(Z)=Z \cdot E_k(1)$), and $\Delta\gamma = -0.5$. The value of $E_k(1)$ is chosen to reproduce the observed size spectrum, assuming that it is dominated by the lightest mass component.

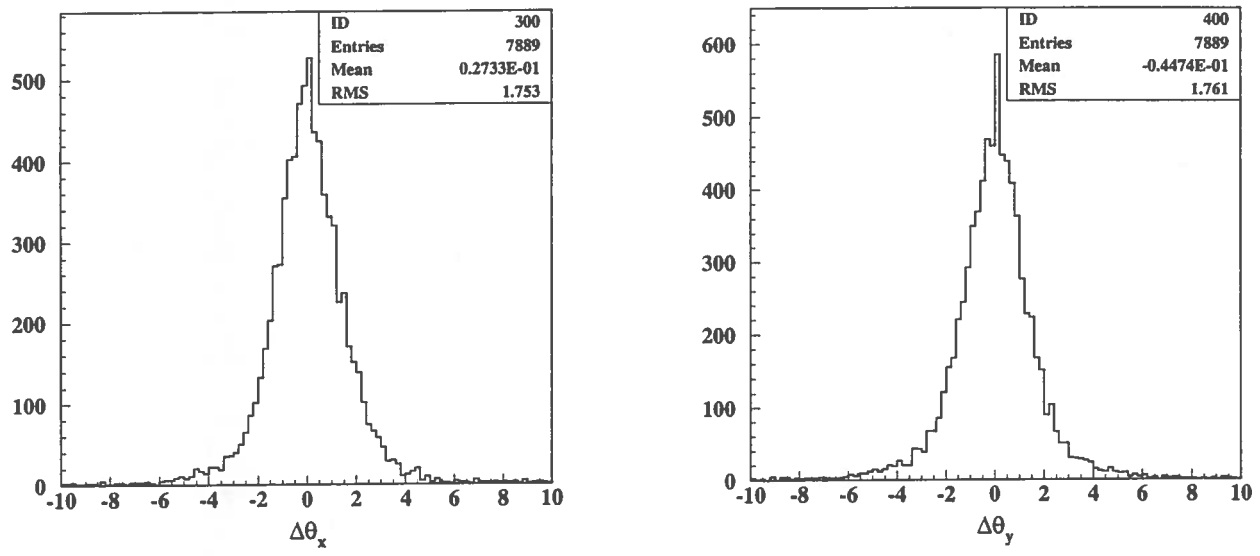

Fig. 1: Distributions of the projected angular difference between the EAS and muon arrival directions measured respectively by EAS–TOP and MACRO.

Table 1: Parameters of the differential spectra $dN/dE = \mathrm{K} \cdot (E/GeV)^{-\gamma}$ of the nuclear components of the composition model used.

Mass group	K $(m^2\ s\ sr\ GeV/nucleus)^{-1}$	γ_1	$E_{knee}\ (GeV)$	γ_2
p	$5.57 \cdot 10^4$	2.86	$2.2 \cdot 10^6$	3.36
He	$9.15 \cdot 10^3$	2.68	$4.4 \cdot 10^6$	3.18
CNO	$1.18 \cdot 10^3$	2.56	$1.5 \cdot 10^7$	3.06
Mg-Si	$1.35 \cdot 10^3$	2.63	$2.6 \cdot 10^7$	3.13
Fe	$1.46 \cdot 10^3$	2.63	$5.7 \cdot 10^7$	3.13

The $N_e - N_\mu$ relation for both composition models and interaction codes is shown in Fig. 2. Most significant are the muon multiplicity distributions obtained for shower sizes below and above the knee of the measured size spectrum, and are shown in Figs. 3 and 4. The high multiplicity tail of the muon number distribution is better reproduced by a composition becoming heavier above the knee, as predicted by the rigidity dependent break, for both interaction models. It is interesting to remark that the DPMJET model solves the systematic deviation of the first point in the $N_e - N_\mu$ plot shown in Fig. 2 (relative to $\approx$ 100 TeV primaries). The measurement concerns the average muon multiplicity $< N_\mu^{det} >$ in fixed size windows and is therefore largely independent of the assumed primary spectra (see paper HE 1.2.24 in these proceedings). This means that for higher primary energies ($\geq$ 1000 TeV, where secondary production at low x_F becomes relevant for the TeV muon yield) both models describe the experimental rates; at lower energies ($<$ 100 TeV, where the fragmentation region is dominant) the DPMJET model is more adequate. A recent work (J. Knapp et al., 1996), aiming to compare different interaction models, confirms that around the knee energy the predictions for TeV muons exhibit differences within 10%. We want also to point out that, qualitatively, the relative difference in the shapes of the muon multiplicity distributions for the two hypotheses about the nature of the knee is only marginally dependent on the details of the chosen input spectra, for a wide class of reasonable mixed compositions. Thus the data support a primary composition becoming heavier above the knee,

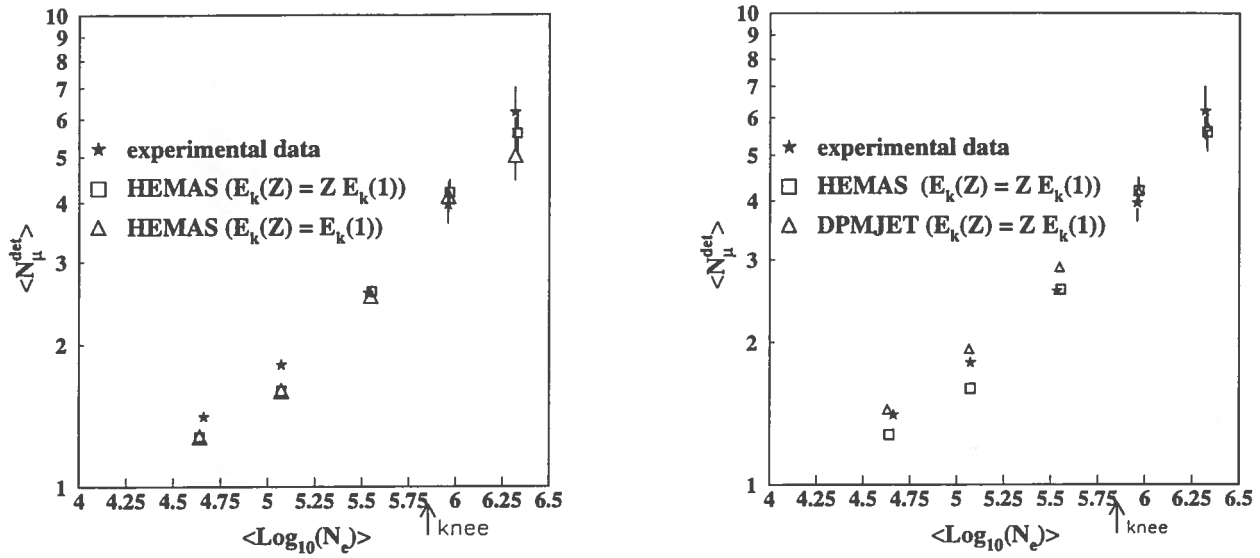

Fig. 2: Correlation between $< N_\mu^{det} >$ and $<Log_{10}N_e>$: comparison between different knee hypotheses (left) and different interaction models (right).

in agreement with the rigidity-dependent model of the knee. We also notice how the analysis of the underground muon fluxes as a function of multiplicity, performed by MACRO alone (Ambrosio et al., 1995 and 1996), is consistent with a rigidity dependent knee. This was first proposed in the frame of the rigidity dependent leakage effect from the Galaxy (P–Z), but other processes can as well be responsible. Different hadron interaction models provide consistent results; this aspect will be further investigated.

REFERENCES

Ambrosio, M. et al., MACRO Collaboration, *Proc. 24rd ICRC*, Rome, **2**, 689 (1995).
Ambrosio, M. et al., INFN/AE-96/28 and 29 (1996), to be published in Phys. Rev. D.
Battistoni, G. et al., *Astropart. Phys.*, **3**, 157 (1995).
Brun, R. et al., CERN report DD/EE/84–1 (1984).
EAS–TOP and MACRO collaborations, *Phys. Rev.*, **D42**, 1396 (1990).
EAS–TOP and MACRO collaborations, *Proc. 23rd ICRC*, Calgary, **2**, 89 (1993).
EAS–TOP and MACRO collaborations, *Phys. Lett.*, **B337**, 376 (1994).
EAS–TOP and MACRO collaborations, *Proc. 24rd ICRC*, Rome, **2**, 710 (1995).
EAS–TOP collaboration, *Proc. 24rd ICRC*, Rome, **2**, 732 (1995).
Forti, C. et al., *Phys. Rev.*, **D42**, 3668 (1990).
Knapp, J., Heck, D. and Schatz, G., Karlsruhe Report FZKA 5828, (1996).
Peters, B., *Proc. 6th ICRC*, Moscow, **3**, 157 (1959).
Ranft, J., *Phys. Rev.*, **D51**, 64 (1995).
Zatsepin, G. T. et al., Izv. Ak. Nauk USSR, SP, 26, 685 (1962).

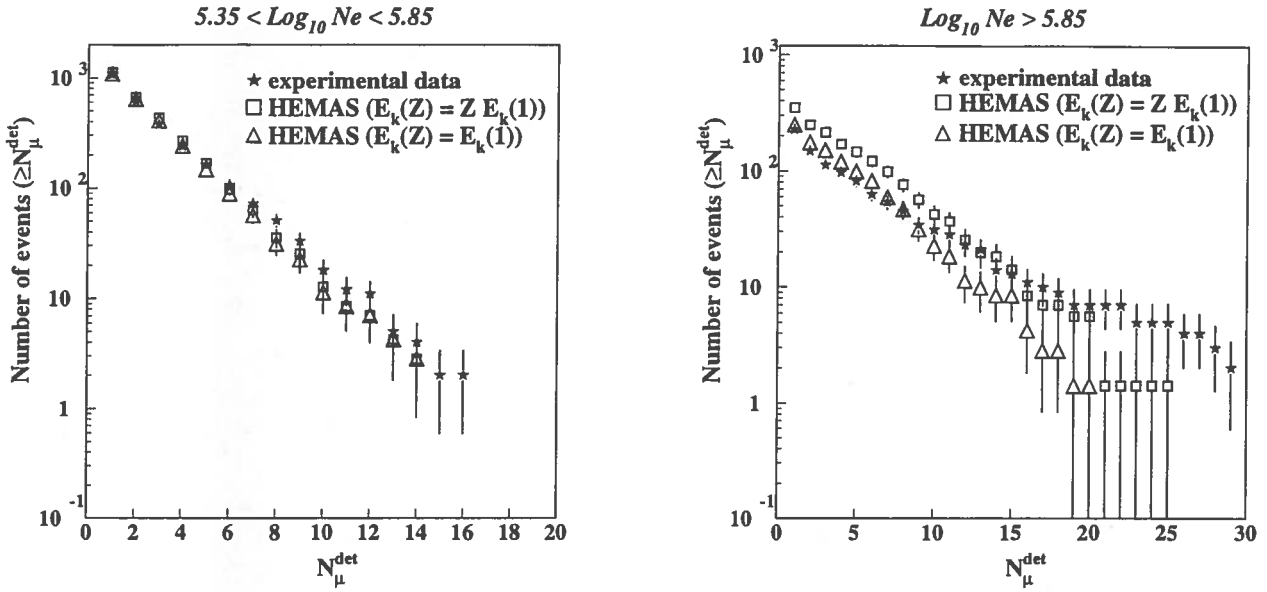

Fig. 3: Measured and expected integral distribution of detected muon multiplicity, for 5.35≤ $Log_{10}N_e$ ≤ 5.85 (left), and $Log_{10}N_e$ > 5.85 (right): comparison between different knee hypotheses.

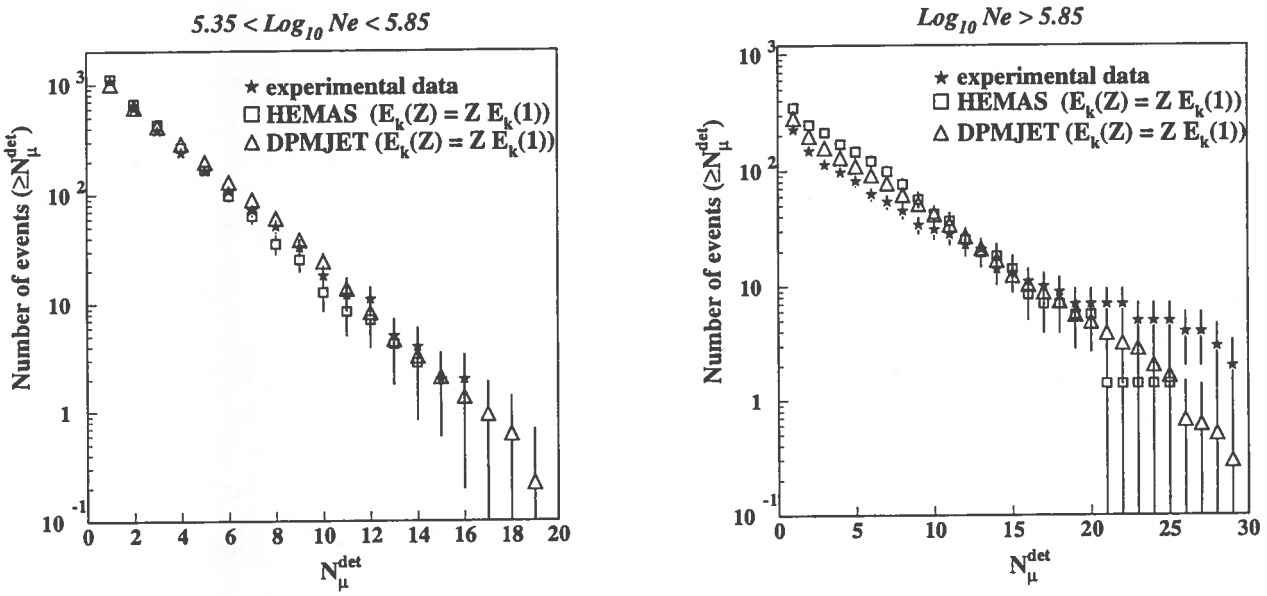

Fig. 4: Measured and expected integral distribution of detected muon multiplicity, for 5.35≤ $Log_{10}N_e$ ≤ 5.85 (left), and $Log_{10}N_e$ > 5.85 (right): comparison between different interaction models.

EXPERIMENTAL STUDY OF HADRONIC INTERACTION MODEL USING COINCIDENT DATA FROM EAS–TOP AND MACRO

EAS-TOP and MACRO Collaborations

INFN/AE–97/47
23 Luglio 1997

ABSTRACT

The measurement of TeV muons in deep underground laboratories and of the e.m. component at the surface allows checks of the hadron interaction models and of the propagation codes used in EAS experiments in a primary energy range 10-50 TeV in which the primary spectra are measured by direct experiments. First results of such measurements between MACRO and EAS-TOP at the Gran Sasso laboratory, providing significant constraints on secondary production cross section in the forward region (x_F >0.2) in this energy range, are here reported. This provides a unique link between the EAS and the cosmic ray direct experiments.

INTRODUCTION

Combined measurements of the e.m. component of EAS at the surface and of the high energy muons detected deep underground are performed by the EAS-TOP and MACRO detectors at the Gran Sasso Laboratories. EAS-TOP is the EAS array (internal area $A_i = 10^5$ m^2, sensitive area $A_s = 350$ m^2) measuring the e.m. shower size at 2000 m a.s.l. (810 g cm^{-}2), while MACRO samples the number of muons (N_μ) at a minimum depth of 3100 m w.e. ($A_s = 6 \times 140$ m^2, E_μ^{th}=1.3 TeV). The two detectors are separated by 1100-1300 m of rock and are located at a relative zenith angle of $\sim 30°$. Details on the detectors and on their performances and the analysis of a first sample of coincident data have been presented elsewhere (EAS-TOP and MACRO, 1990, 1993, 1994, 1995). Concerning the physics results, two classes of events are selected: high energy coincidence events and low energy triggers. For the first class ($E_0 > 100 \div 200$ TeV) full reconstructions are available from both experiments. They are analysed in terms of primary composition, as presented also in these proceedings (EAS-TOP and MACRO, 1997). In the second class, the trigger is provided by at least a muon track in MACRO pointing to a fiducial area ($6.7 \cdot 10^3$ m^2) well internal to the EAS–TOP edges. The analysis is performed in terms of the rates of the number N of detectors fired in EAS–TOP. If N<4, EAS-TOP does not provide trigger, and we define the event as an "anti–coincidence". These events cover a primary energy range from approximately 2 TeV to a few tens of TeV. For N≥4, the energy range of interest becomes intermediate between the anti–coincidences and the high energy triggers. No shower reconstruction is performed by EAS-TOP for N< 7. In the energy intervals covered by the anti–coincidences and low–energy coincidences, the primary spectrum and composition are directly investigated by experiments at the top of the atmosphere or in outer space. It is therefore possible to use these sets of data as an input to test the predictions of different models for the EAS development. In this paper we report the results of a first comparison, where two different interaction models have been tested: 1) In HEMAS (Forti et al., 1990) the basic interaction model is obtained by a proper parametrization of experimental results obtained at accelerators. The nuclear projectiles are treated in the framework of the "semi–superposition model" with the NUCLIB code (Engel et al., 1992). 2) In HEMAS-DPMJET (Battistoni et al., 1995) the shower code of HEMAS is now interfaced to the DPMJET (Ranft, 1995) interaction model. In contrast to the philosophy of the original HEMAS, this is a theoretically inspired model. It is based on the two component Dual Parton Model, including also the mini–jet production as predicted by the lowest order perturbative QCD.

THE SET OF EXPERIMENTAL DATA

For this first analysis of anti–coincidences and low energy triggers, we have used a sample of data

Table 1: Number of experimental detected events for the different trigger classification.

No. of hit modules	No. of detected events	Corrected live time (days)
< 4	6515	153.68
4	204	140.44
5	182	140.44
6	142	140.44
> 7	876	140.44

collected in the period ranging from May 3rd 1993 to September 6th 1994. For the coincidence analysis the data taking corresponds to 140.44 days of operation, taking into account also the dead time of both acquisition systems. We define in the muon event as seen by MACRO a center of gravity of the muon tracks at the level of the floor of the underground laboratory. The event is accepted if the back-extrapolation of the centroid coordinates up to the EAS-TOP height fall inside an *a priori* defined fiducial area in the central and denser part of the EAS-TOP array. Then, if EAS-TOP had a trigger within the time coincidence window, the event is classified according to the number of fired modules. The number of coincidence events thus defined in the considered time period is 1404. Instead, if no trigger with N$\geq$ 4 is provided by EAS-TOP, the event is considered as an "anti–coincidence". After a statistical correction for the dead–time (which acts in opposite ways for coincidences and anti–coincidences), the live time for anti–coincidences is 153.68 days, with 6515 events found. In Table 1 the classification of experimental data is summarized.

MONTE CARLO SIMULATION

The simulation has been performed in the restricted solid angle region useful for the low-energy analysis already described above. All codes use the same muon transport code PROPMU (Lipari and Stanev, 1992). For each Monte Carlo we have generated 5 different mass groups (H, He, CNO, Mg and Fe) with a continuous spectrum, for a corresponding live time of 100 (1000) days below (above) 200 TeV. The generated events have been folded with the detector simulation. A full GEANT (Brun et al., 1984) for the MACRO detector is invoked. For each MACRO event having at least one reconstructed muon, the shower core at EAS-TOP height is recalculated, the trigger simulation is activated and the selection in the fiducial area inside EAS-TOP is applied. At present, both HEMAS and HEMAS-DPMJET have only uni-dimensional simulation of the e.m. shower size, so that a lateral distribution has to be added *a posteriori*. In order to do that, considering that EAS-TOP fits the experimental density distribution using the NKG function, we sample a random value of the effective age parameter distribution of the experimental data. The trigger simulation takes into account the non–poissonian fluctuations of the number of particles hitting the detector modules, as obtained from experimental data, together with ADC response, including the possible saturation. In order to test the accuracy and reliability of the trigger simulation, a detailed cross–check of the procedure here described has been performed by means of more refined methods. The CORSIKA code (Capdevielle et al., 1992) interfaced to EGS (Nelson et al., 1985) has been used to simulate the 3–dimensional e.m. size distribution for different primary energies. Its output has been processed by means of a full GEANT simulation of the EAS-TOP detector. The ratio of the trigger efficiency for N$\geq$4 calculated with the two methods as a function of primary energy has been used to estimate the contribution of trigger simulation to the systematic error of the Monte Carlo predictions: typically, 7% for protons and 15% for He.

ANALYSIS AND RESULTS

As already introduced before, our aim is to look for the differences in the different interaction models. Therefore, we have chosen *a priori* to make use of the results of direct measurements to establish the preferred input spectra and composition. In particular, we use single power law fits to the fluxes of H

Table 2: Comparison between the measured number of events with N modules fired in EAS–TOP (triggered by a muon in MACRO) and the expectations from two interaction models.

No. of EAS–TOP modules fired	N < 4 Antic.	4 ≤ N ≤ 6 Low En. Coinc.	N > 6 High En. Coinc.	N ≥ 0 Total
Exp. Data	4239	376	624	5239
DPMJET Int. Mod.	3502	314	560	4378
HEMAS Int. Mod.	2729	324	600	3653

Table 3: Comparison between the measured average detected muon multiplicity for the anti–coincidence events and the expectations from the two interaction models.

	$< N_\mu >$	$< N_\mu >$(H)	$< N_\mu >$(He)
Exp. Data	1.321 ± 0.003	–	–
DPMJET Int. Mod.	1.310 ± 0.003	1.284	1.424
HEMAS Int. Mod.	1.282 ± 0.003	1.269	1.386

and He as reported by JACEE in 1993 and 1995 (JACEE collab., 1993 and 1995). The data of higher mass components are taken from other experiments (Müller et al., Ivanenko et al., 1991). Our best fits for p and He fluxes provide the following spectra:

$$\begin{aligned} p: &\quad 5.57 \cdot 10^4 \, (E/GeV)^{-2.86} \quad (m^{-2}\, s^{-1}\, sr^{-1}\, GeV^{-1}) \\ He: &\quad 9.15 \cdot 10^3 \, (E/GeV)^{-2.68} \quad (m^{-2}\, s^{-1}\, sr^{-1}\, GeV^{-1}) \end{aligned} \tag{1}$$

The errors on the fit parameters allow an uncertainty of 15 to 20% of these fluxes in the energy range of interest.

The results are shown in Table 2, after the normalization of experimental and simulated data to 100 days of live time. The interaction model in the present configuration is tested in the energy range 2 to 100 TeV. Anti–coincidences are found to be dominated by H and He primaries. As far as the number of simulated events is concerned, the previously quoted uncertainty on the primary flux should be allowed, together with the systematics of the trigger threshold simulation. With such attention, the higher energy rates ($N > 4$) can be described by both models. Even with such care, at the lower energies ($N < 4$) the HEMAS codes underestimates the rate of events much more significantly than DPMJET. In Fig. 1 we show the relative contribution to simulated anti–coincidence events as a function of total primary energy for protons and He nuclei, as calculated by HEMAS and HEMAS-DPMJET. This plot shows the relevant energy range which dominates this class of events and points out how most of the differences in the codes manifest themselves for values of energy/nucleon near the threshold for the production of TeV muons. The contribution of protons to anti–coincidences increases by 18% from HEMAS to HEMAS-DPMJET, while, for He nuclei, the increase is ∼64%. Also the average detected muon multiplicity changes, as shown in Table 3 (where the contribution from H and He is again separated), favouring again the DPMJET interaction model. At this first stage we can conclude that for a fixed minimum muon energy, in the total energy region below <50÷100 TeV, high x_F values become relevant for the TeV muon yield, and this is even more important for primaries heavier than protons. There, the DPMJET model seems more adequate. Considering the basic nucleon-Nucleus interaction, we can quantify the conclusion in terms of of the "spectrum weighted moments" for charged pions: $Z_\pi = \int_0^1 \frac{dN(p+Air \to \pi+X)}{dx} x^{1.7} dx$. As shown in (Battistoni et al., 1995), DPMJET (and other codes based on similar hypotheses) provide larger values with respect to HEMAS: 0.068 in the range 1÷ 100 TeV against 0.061÷0.057 for HEMAS in the same energy range. We can therefore conclude that the

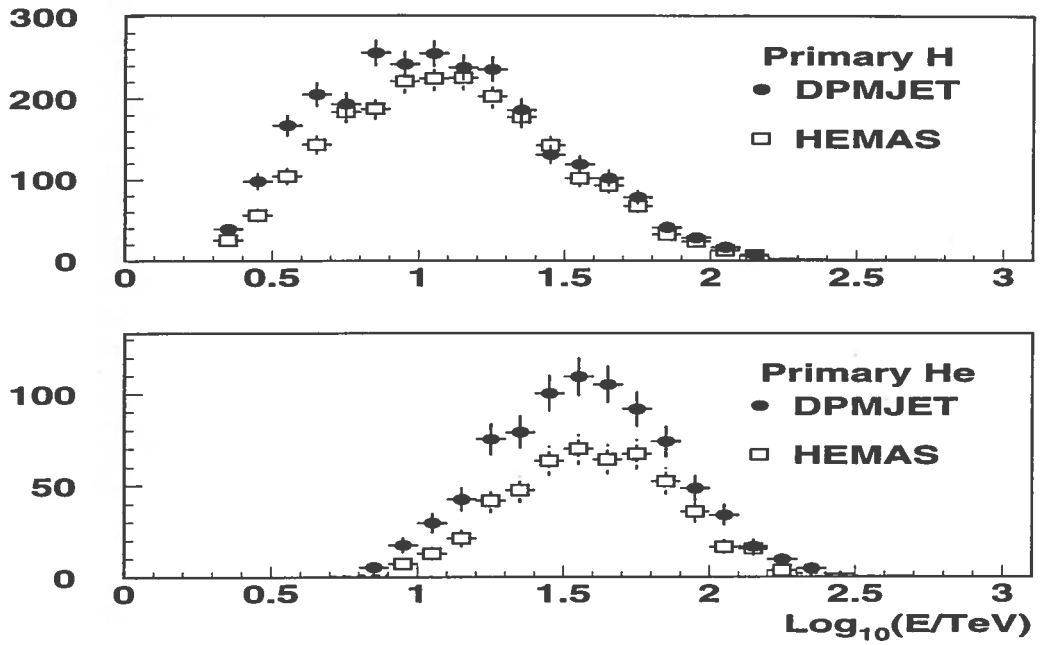

Fig. 1: Relative contribution to simulated anticoincidence events as a function of total primary energy for protons and He nuclei, as calculated by HEMAS and HEMAS-DPMJET

coincident data collected by EAS-TOP and MACRO in the region below 50÷100 TeV, where direct measurements on primary fluxes are available, can be used to discriminate the prediction of different hadronic interaction models. A minimum value of $Z_\pi(E < 100\ TeV)$ ~0.068 is required to obtain a reasonable agreement with the present primary fluxes.

REFERENCES

Battistoni, G. et al., *Astropart. Phys.*, **3**, 157 (1995).
Brun, R. et al., CERN report DD/EE/84-1 (1984).
Capdevielle, J. N. et al., "the Karlsruhe extensive air shower simulation code CORSIKA", KFK Report 4998 (1992).
EAS-TOP and MACRO Collaborations, *Phys. Rev.*, **D42**, 1396 (1990).
EAS-TOP and MACRO Collaborations, *Proc. 23rd ICRC,* Calgary, **2**, 89 (1993).
EAS-TOP and MACRO Collaborations, *Phys. Lett.*, **B337**, 376 (1994),
EAS-TOP and MACRO Collaborations, *Proc. 24rd ICRC,* Rome, **2**, 710 (1995).
EAS-TOP and MACRO Collaborations, *Proc. 25rd ICRC,* Durban, OG 6.1.14 (1997).
Engel, J. et al., *Phys. Rev.* **D46**, 5013 (1992).
Forti, C. et al., Phys. Rev. **D42**, 3668 (1990).
Ivanenko, I. P. et al., *Proc. 22nd ICRC.*, Dublin, **2**, 17 (1991).
JACEE Collaboration, *Proc. 23rd ICRC,* Calgary, **2**, 25 (1993).
JACEE Collaboration, *Proc. 24rd ICRC,* Rome, **2**, 728 (1995).
Müller, D. et al., *Ap.J.*, **374**, 356 (1991).
Nelson, W. R. et al., SLAC Report 265 (1985).
Ranft, J. *Phys. Rev. D*, **51**, 64 (1995).

The MACRO Collaboration

M. Ambrosio[12], R. Antolini[7], G. Auriemma[14,a], R. Baker[11], A. Baldini[13], G. C. Barbarino[12], B. C. Barish[4], G. Battistoni[6,b], R. Bellotti[1], C. Bemporad[13], P. Bernardini[10], H. Bilokon[6], V. Bisi[16], C. Bloise[6], C. Bower[8], S. Bussino[14], F. Cafagna[1], M. Calicchio[1], D. Campana[12], M. Carboni[6], M. Castellano[1], S. Cecchini[2,c], F. Cei[13,d], P. Celio[14], V. Chiarella[6], A. Corona[14], S. Coutu[11], G. De Cataldo[1], H. Dekhissi[2,e], C. De Marzo[1], I. De Mitri[9], M. De Vincenzi[14,f], A. Di Credico[7], O. Erriquez[1], C. Favuzzi[1], C. Forti[6], P. Fusco[1], G. Giacomelli[2], G. Giannini[13,g], N. Giglietto[1], M. Goretti[4,14], M. Grassi[13], L. Gray[7], A. Grillo[7], M. Grippa[6,b], F. Guarino[12], P. Guarnaccia[1], C. Gustavino[7], A. Habig[3], K. Hanson[11], A. Hawthorne[8], R. Heinz[8], E. Iarocci[6,h], E. Katsavounidis[4], E. Kearns[3], S. Kyriazopoulou[4], E. Lamanna[14], C. Lane[5], D. S. Levin[11], P. Lipari[14], N. P. Longley[4,m], M. J. Longo[11], F. Maaroufi[2,e], G. Mancarella[10], G. Mandrioli[2], S. Manzoor[2,n], A. Margiotta Neri[2], A. Marini[6], D. Martello[10], A. Marzari-Chiesa[16], M. N. Mazziotta[1], C. Mazzotta[10], D. G. Michael[4], S. Mikheyev[7,i], L. Miller[8], P. Monacelli[9], T. Montaruli[1], M. Monteno[16], S. Mufson[8], J. Musser[8], D. Nicoló[13,d], R. Nolty[4], C. Okada[3], C. Orth[3], G. Osteria[12], O. Palamara[10], S. Parlati[7], V. Patera[6,h], L. Patrizii[2], R. Pazzi[13], C. W. Peck[4], S. Petrera[9,10], P. Pistilli[14,f], V. Popa[2,l], V. Pugliese[14], A. Rainó[1], J. Reynoldson[7], F. Ronga[6], U. Rubizzo[12], A. Sanzgiri[15], C. Satriano[14,a], L. Satta[6,h], E. Scapparone[7], K. Scholberg[3,4], A. Sciubba[6,h], P. Serra-Lugaresi[2], M. Severi[14], M. Sioli[2], M. Sitta[16], P. Spinelli[1], M. Spinetti[6], M. Spurio[2], R. Steinberg[5], J. L. Stone[3], L. R. Sulak[3], A. Surdo[10], G. Tarlé[11], V. Togo[2], C. W. Walter[4] and R. Webb[15]

1. Dipartimento di Fisica dell'Università di Bari and INFN, 70126 Bari, Italy
2. Dipartimento di Fisica dell'Università di Bologna and INFN, 40126 Bologna, Italy
3. Physics Department, Boston University, Boston, MA 02215, USA
4. California Institute of Technology, Pasadena, CA 91125, USA
5. Department of Physics, Drexel University, Philadelphia, PA 19104, USA
6. Laboratori Nazionali di Frascati dell'INFN, 00044 Frascati (Roma), Italy
7. Laboratori Nazionali del Gran Sasso dell'INFN, 67010 Assergi (L'Aquila), Italy

8. Depts. of Physics and of Astronomy, Indiana University, Bloomington, IN 47405, USA
9. Dipartimento di Fisica dell'Università dell'Aquila and INFN, 67100 L'Aquila, Italy
10. Dipartimento di Fisica dell'Università di Lecce and INFN, 73100 Lecce, Italy
11. Department of Physics, University of Michigan, Ann Arbor, MI 48109, USA
12. Dipartimento di Fisica dell'Università di Napoli and INFN, 80125 Napoli, Italy
13. Dipartimento di Fisica dell'Università di Pisa and INFN, 56010 Pisa, Italy
14. Dipartimento di Fisica dell'Università di Roma "La Sapienza" and INFN, 00185 Roma, Italy
15. Physics Department, Texas A&M University, College Station, TX 77843, USA
16. Dipartimento di Fisica Sperimentale dell'Università di Torino and INFN, 10125 Torino, Italy
a Also Università della Basilicata, 85100 Potenza, Italy
b Also INFN Milano, 20133 Milano, Italy
c Also Istituto TESRE/CNR, 40129 Bologna, Italy
d Also Scuola Normale Superiore di Pisa, 56010 Pisa, Italy
e Also Faculty of Sciences, University Mohamed I, B.P. 424 Oujda, Morocco
f Also Dipartimento di Fisica, Università di Roma Tre, Roma, Italy
g Also Università di Trieste and INFN, 34100 Trieste, Italy
h Also Dipartimento di Energetica, Università di Roma, 00185 Roma, Italy
i Also Institute for Nuclear Research, Russian Academy of Science, 117312 Moscow, Russia
l Also Institute for Space Sciences, 76900 Bucharest, Romania
m Swarthmore College, Swarthmore, PA 19081, USA
n RPD, PINSTECH, P.O. Nilore, Islamabad, Pakistan

Acknowledgements.

We gratefully acknowledge the support of the director and of the staff of the Laboratori Nazionali del Gran Sasso and the invaluable assistance of the technical staff of the Institutions participating in the experiment. We thank the Istituto Nazionale di Fisica Nucleare (INFN), the U.S. Department of Energy and the U.S. National Science Foundation for their generous support of the MACRO experiment. We thank INFN, ICTP (Trieste) and NATO for providing fellowships and grants (FAI) for non Italian citizens.

EAS-TOP COLLABORATION

M.Aglietta[a,b], B.Alessandro[b], P.Antonioli[c], F.Arneodo[d,e], L.Bergamasco[b,f], M.Bertaina[b,f], C.Castagnoli[a,b], A.Castellina[a,b], A.Chiavassa[b,f], G.Cini Castagnoli[b,f], B.D'Ettorre Piazzoli[g], G.Di Sciascio[g], W.Fulgione[a,b], P.Galeotti[b,f], P.L.Ghia[b,f], M.Iacovacci[g], G.Mannocchi[a,b], C.Morello[a,b], G.Navarra[b,f], O.Saavedra[b,f], G.C.Trinchero[a,b], P.Vallania[a,b], S.Vernetto[a,b], C.Vigorito[b,f]

a) Istituto di Cosmo-Geofisica del CNR, Corso Fiume 4, 10133 Torino, Italy
b) Istituto Nazionale di Fisica Nucleare, Via Pietro Giuria 1, 10125 Torino, Italy
c) Istituto Nazionale di Fisica Nucleare, Via Irnerio 46, 40126 Bologna, Italy
d) Dipartimento di Fisica dell' Università dell'Aquila, Via Vetoio, 67010 L'Aquila, Italy
e) INFN Laboratori Nazionali del Gran Sasso, S.S. 17 bis, 67010 Assergi (AQ), Italy
f) Dipartimento di Fisica Generale dell' Università, Via P. Giuria, 1, 10125 Torino, Italy
g) Dipartimento di Scienze Fisiche dell' Università and INFN, Mostra D'Oltremare, 80125 Napoli, Italy